Concrete Science and Engineering, Vol. 1, March 1999, pp 15-25

RESEARCH PAPERS

Effect of mechanical clamping on the pull-out response of hooked steel fibers embedded in cementitious matrices

Jamil M. Alwan[1], Antoine E. Naaman[2] and Patricia Guerrero[3]
(1) Safety & Biomechanics CAE Dept., Dearbon, MI, 48121, USA
(2) Dept. of Civil & Environmental Engineering, University of Michigan, Ann Arbor, MI, 48109-2125, USA
(3) Universidad del Valle, Faculdad de Ingenieria, Ciudad Universitaria Melendez, Apartado 25360, Cali, Colombia

ABSTRACT

The main objective of this research is to develop a rational model to predict the pull-out load versus fiber end slip response of hooked steel fibers as they are pulled out from quasi-brittle matrices such as cement and ceramics. The pull-out response of smooth steel fibers is generally affected by two interfacial bond properties; the elastic adhesive-type bond parameter and the frictional bond parameter. In the case of deformed steel fibers, a third parameter is present which is due to the geometry of the fiber. For hooked steel fibers, for instance, this parameter is the mechanical clamping action due to the hook geometry. In this study, a new analytical solution is derived to determine the mechanical contribution of the hook in a general fiber pull-out model. The model is based on the concept of a frictional pulley along which the rotational resistance of up to two plastic hinges is integrated. The mechanical contribution of the hook is a function of the cold work needed to straighten the fiber as it is being pulled-out from its print. A limited experimental study was also carried out to identify basic variables and parameters, to ascertain their influence on the mechanical contribution of the hook, and compare analytical predictions with experimental observations. Variables that were studied in the experimental program include fiber embeddment length, matrix strength, and the fiber-matrix interfacial bond properties. The model predictions were compared to the experimental results and good agreement was observed. The model can be used as a design tool to optimize the energy absorbing properties of fiber reinforced cement and ceramic composites.

INTRODUCTION

Cementitious materials such as mortar and concrete are known for their weakness in resisting tensile stresses. Fiber reinforcement makes up for this deficiency. Fiber reinforced composites resist tensile forces through a composite action whereby part of the tensile forces is resisted by the cementitious matrix while the balance is taken by the fibers. The transmission of forces between the fiber and the matrix is done through bond which characterizes the interface mechanics between the fiber and the surrounding matrix.

The components of bond can be classified as follows: 1) the physical and/or chemical adhesion between fiber and matrix, 2) the frictional resistance, 3) the mechanical component (coming from a particular geometry of the fiber be it deformed, crimped, or hooked fibers), and 4) the fiber-to fiber interlock. Several prior investigations, analytical or experimental, have dealt with some of these components. However, to the authors knowledge, only one prior study has addressed the mechanical component of bond of crimped fibers (Chanvillard [4, 5]) and this one which deals with the mechanical contribution of the hook in hooked fibers.

OBJECTIVE

The present investigation is focused on understanding the contribution of the mechanical component of bond in hooked steel fibers and modeling such contribution in the general pull-out response of the fibers from a cement or ceramic based matrix. An interactive approach between experiments and modeling was followed initially, to ascertain the importance of basic variables and parameters considered in the model. This was important not only to identify qualitatively these variables but also to model their influence quantitatively.

EXPERIMENTAL PROGRAM

The experimental investigation focused on isolating the contribution of the hook (*i.e.* load and slip) of a steel fiber through a series of pull-out tests of a single hooked

Table 1 – Parameters of hooked steel fibers used							
Fiber Type	Name	Original Length (mm)	Embedded Length (mm)	Diameter (mm)	Perimeter Strength (mm)	Yield Strength (MPa)	Ultimate (MPa)
1	30/50	30	12.5	0.5	1.5708	896-1,172	4,185
2	50/50	50	25.0	0.5	1.5708	896-1,172	4,185

1 ksi = 6.89 MPa.

between fiber and matrix.

Commercially available round hooked steel fibers (Dramix) were used in the tests. They were 0.5 mm in diameter and either 30 mm or 50 mm in length. Additional information on yield and tensile strength as provided by the manufacturer are summarized in Table 1.

Table 2 – Composition of matrix mixtures by weight							
Mix Type	Cement	Sand 50-70	Fine Sand-270	Metakaolin	Fly Ash	*w/c	Symbol
1	1.0	1.0	0.0	0.0	20%	0.5	M1
2	1.0	0.0	2.0	0.0	20%	1.0	M2
3	1.0	0.0	2.0	10%	10%	0.9	M3

The three matrix fillers included: (1) the addition of fly ash; (2) the use of fine sand (dust-like sand ASTM-270); and (3) the addition of metakaoline. Table-1 summarizes the three basic matrix mixtures used in this study. Note that the water content of mix M2 and M3 is very high and was necessitated by the very fine sand used.

Table 3 – Nomenclature of pull-out samples			
Sample	Index-1 Mix Type	Index-2 Fiber type	Index-3 Repetitivity
M1H30A	Mix1	30/50	A
M1H30B	Mix1	30/50	B
M1H30C	Mix1	30/50	C
M1H50A	Mix1	50/50	A
M1H50B	Mix1	50/50	B
M1H50C	Mix1	50/50	C
M2H30A	Mix2	30/50	A
M2H30B	Mix2	30/50	B
M2H30C	Mix2	30/50	C
M2H50A	Mix2	50/50	A
M2H50B	Mix2	50/50	B
M2H50C	Mix2	50/50	C
M3H30A	Mix3	30/50	A
M3H30B	Mix3	30/50	B
M3H30C	Mix3	30/50	C
M3H50A	Mix3	50/50	A
M3H50B	Mix3	50/50	B
M3H50C	Mix3	50/50	C

Specimen identification

Three indices were used to identify the test specimens. The first index indicates the type of matrix (M1, M2, or M3), the second index the type of fiber (H30 or H50), and the third index (A, B, or C) repetitivity for averaging. Table-3 summarizes the pull-out sample nomenclature.

Specimen casting and curing

The steel hooked fibers were embedded in half "dog bone" shaped cementitious specimens (Fig. 1). At first, the fibers were placed in polyurethane rectangular prisms. These prisms allowed accurate positioning of the fibers and insured the desired embedded length. They were placed securely in one side of the plexiglas mold while the matrix was poured. The Plexiglas molds were first oiled to facilitate demolding after matrix hardening. After demolding, the polyurethane prisms were removed thus exposing the fiber end for future pull-out.

After demolding, the specimens were cured in water for seven days at room temperature, then left in laboratory environment (21°C, 70% RH) until tested.

steel fiber from a cementitious matrix. It has been observed in the past that the mechanical clamping of the hook increases the pull-out load as well as the pull-out energy significantly [1-5], and that for normal to high strength matrices the hook of the fiber straightened out during the pull-out process.

The test parameters included hooks from two different fibers, embedded lengths of fibers (either 12.5 mm or 25 mm) and matrix composition through addition of fillers to improve the compaction of the matrix in the interfacial zone

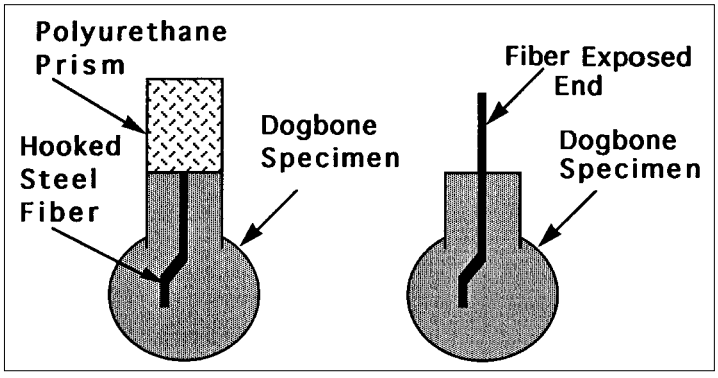

Fig. 1 - Pull-out specimen preparation.

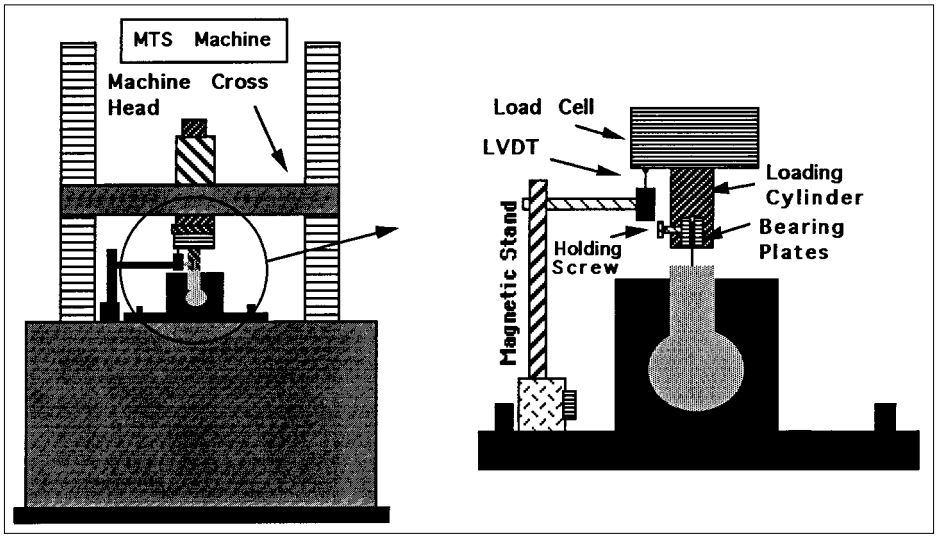

Fig. 2 - Test Setup.

Test Setup

A simple experimental pull-out test setup was used in this study (Fig. 2). The setup comprisd a supporting fixture attached to the bed of the testing machine, and a loading cylinder attached to the load cell. The cylinder type jaw was used to insure better alignment in applying the load along the fiber axis. An MTS hydraulic testing machine with a 100 lbs. load cell was used under displacement control. The fiber end displacement was measured by an external LVDT.

Experimental observation

In order to determine reference interfacial properties, round smooth steel fibers (*i.e.* hook cut off) of 0.5 mm in diameter were pulled out separately from dog bone specimens made of the three different mixes discussed earlier. Two different embedded lengths of 12.5 mm and 25 mm were used as well. Fig. 3 shows the average pull-out load versus fiber end displacement curves for the 12.5 mm embedded length. It can be observed that the maximum pull-out load of smooth fibers is directly related to the type of matrix. Using the assumption that the maximum pull out load occurs at the onset of complete debonding (in reality the maximum load could occur somewhere between 80% to 100% of fiber debonding), the maximum (initial) frictional bond shear stress can be estimated from equilibrium as:

$$\tau_f = P_{max}/(\pi d_f l_f) \quad (1)$$

where, P_{max} = Maximum pull-out load, d_f = Fiber diameter, l_f = Fiber embedded length.

Computing τ_f for the three matrix mixtures used yields the following: τ_f = 335 psi for Mix #1; τ_f = 251 psi for Mix # 2; and finally τ_f = 190 psi for Mix #3.

Figs. 4 to 10 show plots of the pull-out load versus fiber end displacement curves of hooked steel fibers as they are pulled-out from the three types of matrices (*i.e.* Mixes 1, 2, and 3). For all three mixes, the maximum pull-out load averaged from 32.5 to 37 lb. (144-164 N) for an embedded length of 12.5 mm and from 40 to 47.5 lb.(178-211 N) for an embedded length of 25 mm. In all cases the hook end of the fiber was straightened during fiber pull-out. This straightening mechanism contributes significantly to the pull-out resistance through plastic

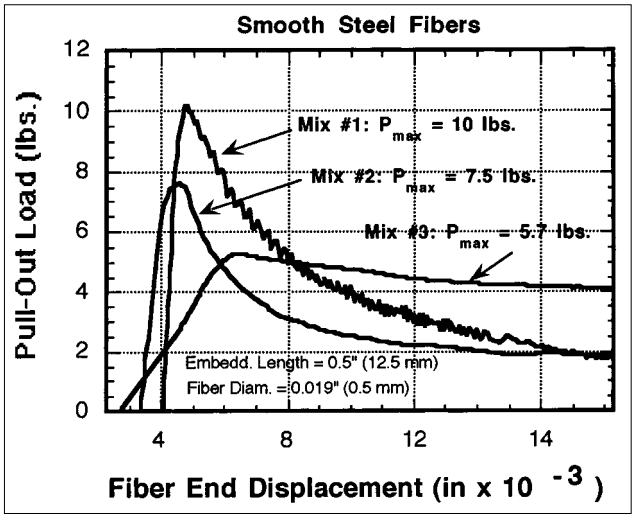

Fig. 3 Pull-out curves of smooth steel fibers from three different cementitious matrices.

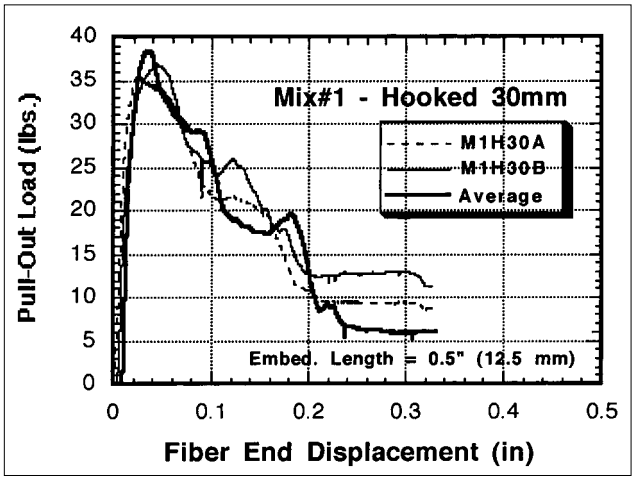

Fig. 4 - Pull-out curves of 1/2 " hooked steel fibers from mix #1 matrix.

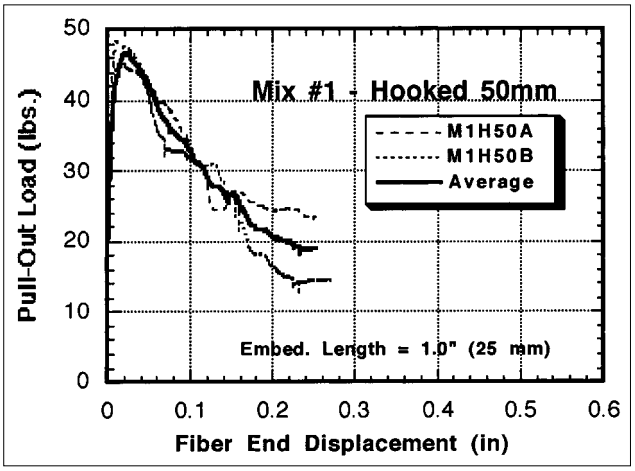

Fig. 5- Pull-out curves of 1" hooked steel fibers from mix #1 matrix.

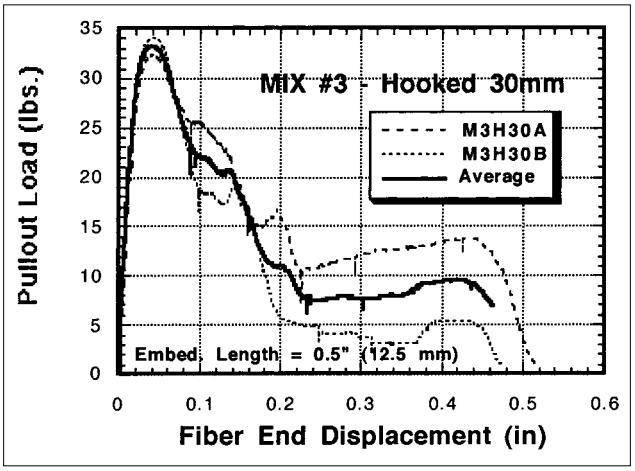

Fig. 8- Pull-out curves of 1/2" hooked steel fibers from mix #3 matrix.

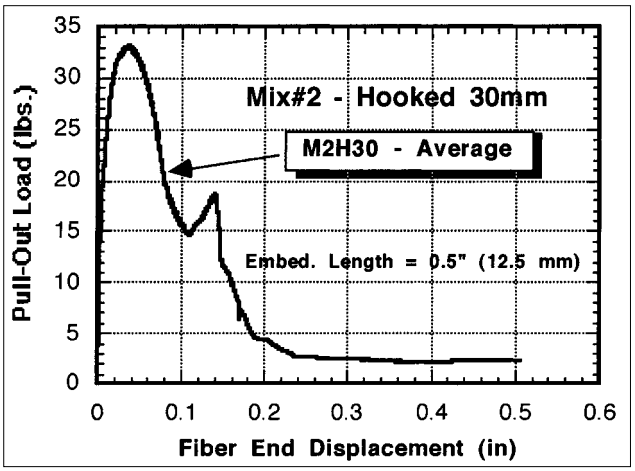

Fig. 6- Typical pull-out curves of 1/2 " hooked steel fibers from mix #2 matrix.

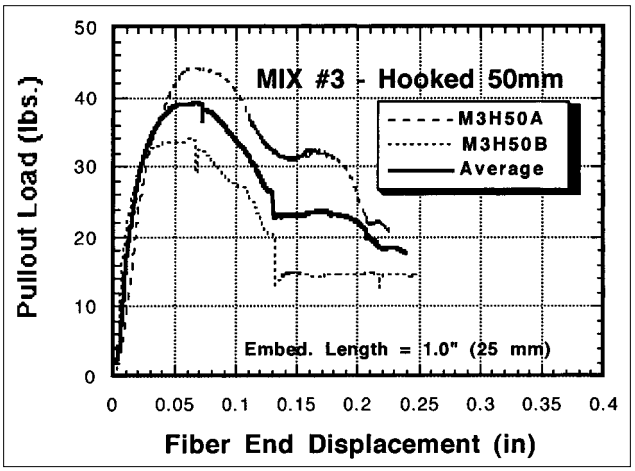

Fig. 9 - Pull-out curves of 1" hooked steel fibers from mix #3 matrix.

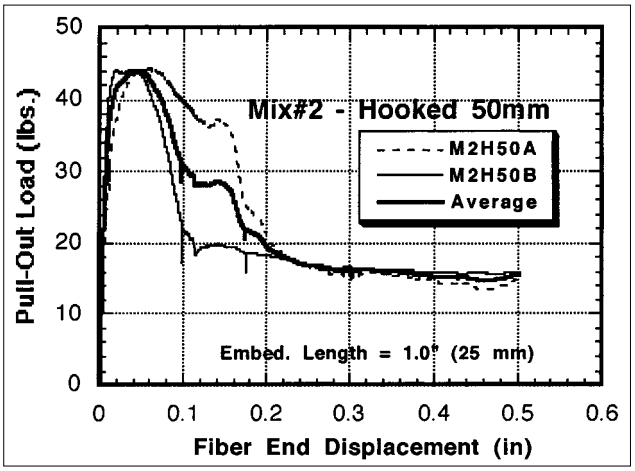

Fig. 7- Pull-out curves of 1" hooked steel fibers from mix #2 matrix.

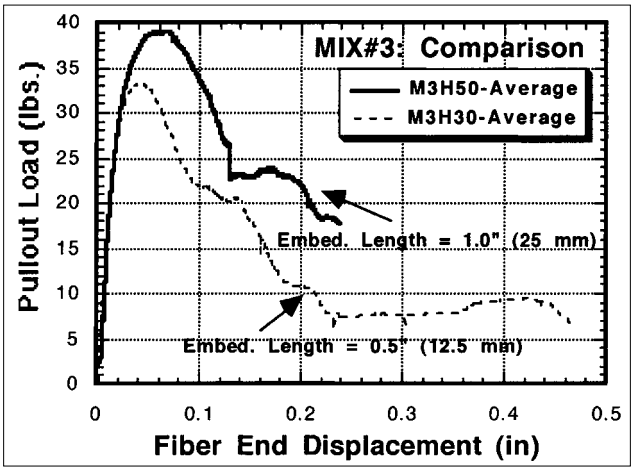

Fig. 10 - Comparison of average pull-out curves of 1/2" & 1" hooked steel fibers from mix #3 matrix.

rotation of the fiber cross section at that location. The hook contribution should be about constant in all cases, provided complete straightening of the fiber hooked end prevails without any matrix failure [11-14].

To examine this inference, the maximum pull-out load at the onset of complete debonding of smooth fibers was subtracted from the maximum pull out load of hooked fibers of the same embedded length and matrix mix design. Table 4 summarizes the results obtained.

It is clear that the mechanical contribution of the hook

Table 4 – Hook end mechanical contribution to the maximum pull-out load						
	Pull-Out Load (lb.) (l_f = 0.5")	Pull-Out Load (lb.) (l_f = 0.5")	Hook End Load (lb.) (l_f = 0.5")	Pull-Out Load (lb.) (l_f = 1.0")	Pull-Out Load (lb.) (l_f = 1.0")	Hook End Load (lb.) (l_f = 1.0")
Fiber Type	Smooth	Hooked	Difference	Smooth	Hooked	Difference
Mix #1	10.0	37.0	27.0	20	47.5	27.5
Mix #2	7.5	34.0	26.5	15	44	29.0
Mix #3	5.7	32.5	26.8	11.4	40	28.0
		Avg. =	**26.7**		**Avg. =**	**28.3**

(placed at the end of a fiber) to the maximum pull-out load is the same in all cases (about 27-28 lb.) and that it is independent of the matrix strength and fiber embedded length. The hook contribution should depend on the fiber properties and the hook geometry (*i.e.* inclination angle, fiber diameter, and hook length).

In comparing Figs. 3 and 6, a couple of observations are in order: 1) for smooth fibers the descending branch is smooth characterizing frictional pull-out while for hooked fibers the descending branch seems to undergo a second peak at a fiber end displacement between 0.1 in. and 0.2 in. (2.5 to 5 mm); 2) the load after peak for smooth fibers decreases at a very fast rate practically becoming insignificant after small end slips of about 2.5 mm.

ANALYTICAL FORMULATION

Experimental observations suggest that the pull-out process of a hooked steel fiber is very similar to that of a smooth fiber up to the load level that causes complete interfacial debonding of the fiber. Also beyond that point, taken at the peak load, it seems that the mechanical contribution of the hook is primarily responsible for the pull-out resistance. Naaman et al [1-3] have formulated a mathematical model for the pull-out response of smooth steel fibers based on the interfacial bond stress versus local slip relationship. In their model, they classified three different stages of pull-out:

1) The elastic stage prior to the critical load, P_{crit}, where P_{crit} represents the limit load, which, if exceeded, triggers debonding.

2) The partial debonding stage, where the pull-out load is resisted partially by elastic shear stresses and partially by interfacial frictional stresses. This stage prevails until the whole fiber-matrix interface is completely debonded.

3) The frictional pull-out stage, in which the fiber is rigidly displaced from the matrix through its print and the pull-out resistance is fully supplied by decaying interfacial frictional stresses. This stage occurs after the peak load.

The first two stages of the smooth fiber pull-out scenario (*i.e.* elastic and partial debonding) apply to hooked steel fibers as well (Figs. 11 a, and 12); however, the frictional pull-out stage (Fig. 11d) is preceded by a mechanical clamping stage (Figs. 11b, and 11c). In that stage, the fiber hooked end is subjected to cold work that causes the hook to deform and straighten through the fiber print (tunnel) as it is being pulled out from the matrix. The positions of the sections of plastic hinges, whereby the steel fiber undergoes large deformations, change through the process. For instance, there are two plastic hinge locations at the beginning of this stage (Fig. 11b), and then only one remains afterwards (Fig. 11c). In both cases however, the plastic deformation of the fiber causes a direct increase in the value of the fiber pull-out load.

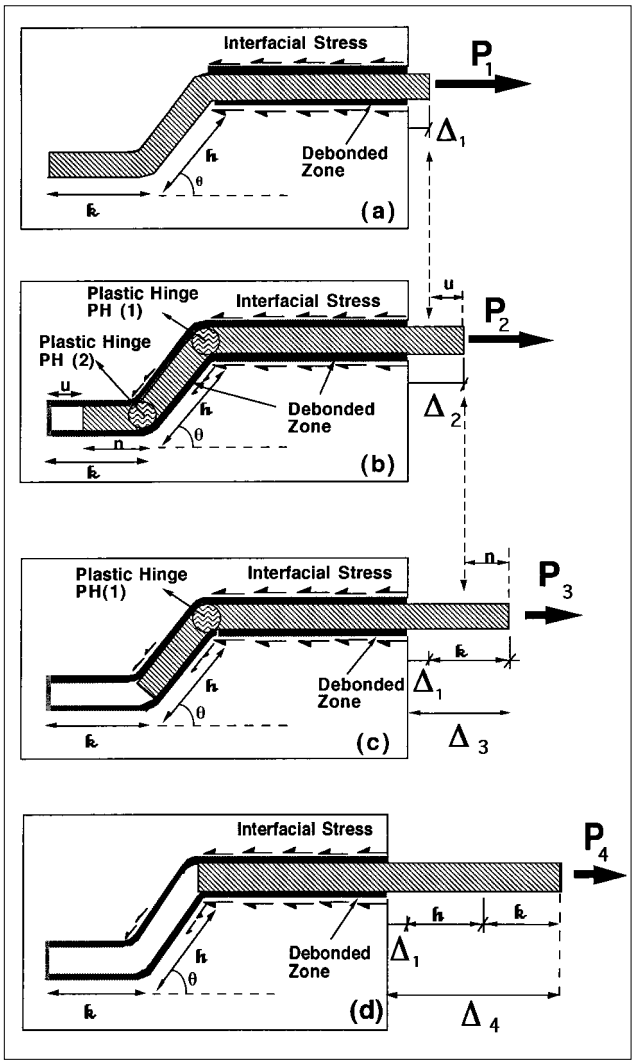

Fig. 11 - a) Hooked steel fiber at onset of complete debonding, b) hooked steel fiber during mechanical interlock with two plastic hinges, c) mechanical interlock with one plastic hinge, d) Hooked Steel fiber at onset of frictional pull-out.

Theoretical Model

Examining the theoretical pull-out curve in Fig.12, it can be observed that the pull-out load vs. fiber end displacement relationship, up to full debonding at load level $\mathbf{P_1}$ and the corresponding fiber end displacement Δ_1, can be predicted using the mathematical model developed by Naaman *et al.* [2, 3] for smooth fibers (Appendix II). After complete debonding, the horizontal portion of the fiber would still be subjected to interfacial frictional stresses and the hooked end of the fiber undergoes cold work deformations through two plastic hinges as indicated in Fig.11b. The corresponding increase in the pull-out load value, due to the cold work from both plastic hinges, would then be added to $\mathbf{P_1}$ resulting in a plateau load ($\mathbf{P_2}$ or $\mathbf{P_3}$). This plateau value remains until the fiber is pulled by an additional distance "k" after which there would be only one active plastic hinge in the hooked end (Fig. 11c), and the pull-out load would drop to $\mathbf{P_4}$. The new load at $\mathbf{P_4}$ would then be held constant as the fiber is pulled-out by an additional distance "h" after which the pull-out load vs. fiber end displacement can then be described by the frictional pull-out model of smooth fibers by Naaman *et al.* [2,]. Hence the only values that need to be defined are the contribution of plastic hinges to the pull-out loads $\mathbf{P_3}$ and $\mathbf{P_4}$, and their corresponding fiber end displacements Δ_3 and Δ_4, respectively. The values of Δ_3 and Δ_4 can be found from Figs. 11(c) and (d) as: $\Delta_3 = \Delta_1 + k$, and $\Delta_4 = \Delta_3 + h$. The values of "k" and "h" are given from the geometry of the hook.

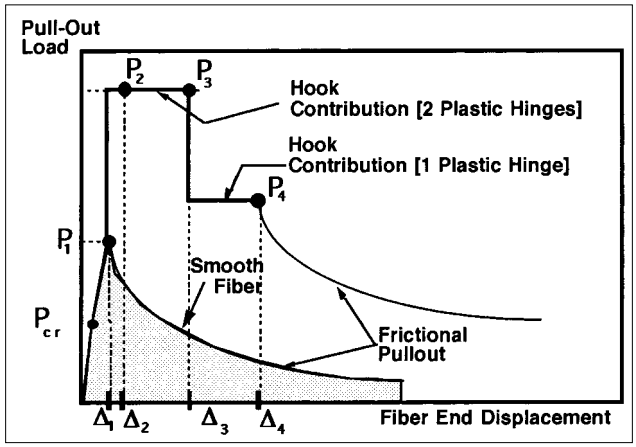

Fig. 12 - Schematic sketch of the theoretical pull-out curve of a hooked steel fiber from a cementitious matrix.

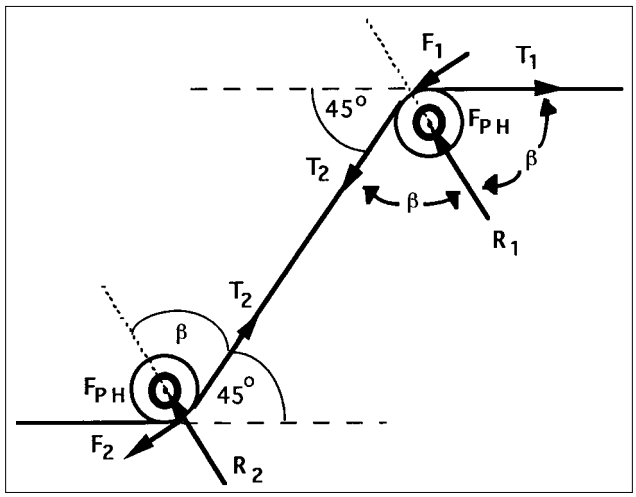

Fig. 13 - Line sketch of the frictional pulley model.

Mathematical Derivation

It was stated in the previous section that the first pull-out load plateau at $\mathbf{P_3}$ (Fig. 12) due to the two plastic hinges can be estimated by:

$$\mathbf{P_3} = \mathbf{P_1} + \Delta P' \tag{2}$$

where, $\mathbf{P_1}$ = Pull-out load at onset of complete debonding and $\Delta P'$ = Pull-out load due to two plastic hinges.

Similarly, the second pull-out load plateau at $\mathbf{P_4}$ (Fig. 12) can be defined as:

$$\mathbf{P_4} = \mathbf{P_1} + \Delta P'' \tag{3}$$

where, $\Delta P''$ = Pull-out load due to one plastic hinge.

In order to determine the values of $\Delta P'$ and $\Delta P''$, an equivalent pulley model is used (Fig. 13). The model simply consists of two frictional pulleys. Both Pulleys have rotational and tangential components of friction resisting the pull-out process. The rotational friction component correspond to the cold work needed for straightening the steel fiber at the plastic hinge location, and is represented by F_{PH} in Fig. 13. The tangential friction component represents the work of Coulomb friction between the steel fiber and the matrix at the contact corner during the straightening of the fiber; it is represented by F_1 and F_2 in Fig. 13. T_1 and T_2 represent the chord tension before and after the first pulley respectively. Moreover, since the hook angle is 45° on both sides it can be stated that:

$$T_1 = \Delta P' \tag{4}$$

and that,

$$T_2 = \Delta P'' \tag{5}$$

R_1 and R_2 in Fig. 13 represent the reaction forces at the pulley centers; they are directly related to F_1 and F_2 through the kinetic coefficient of friction between the fiber and the matrix, μ.

From equilibrium, the following can be stated:

$$T_1 = 2F_{PH} + F_1 + F_2 \tag{6}$$

and,

$$T_2 = F_{PH} + F_2 \tag{7}$$

hence,

$$T_1 = T_2 + F_{PH} + F_1 \quad (8)$$

Moreover,

$$F_1 = R_1 \cdot \mu \quad (9)$$

but,

$$R_1 = T_1 \cdot \cos\beta + T_2 \cdot \cos\beta \quad (10)$$

Substituting (10) in (9), we get:

$$F_1 = (\mu) \cdot [T_1 \cdot \cos\beta + T_2 \cdot \cos\beta] \quad (11)$$

or,

$$F_1 = (\mu) \cdot (\cos\beta) \cdot [T_1 + T_2] \quad (12)$$

Similarly,

$$F_2 = (\mu) \cdot (\cos\beta) \cdot [T_2] \quad (13)$$

Substituting (13) in (7), yields:

$$T_2 = F_{PH} + (\mu) \cdot (\cos\beta) \cdot [T_2] \quad (14)$$

Thus by solving (14) for T_2, we get:

$$T_2 = \frac{F_{PH}}{\left[1 - \mu \cdot \cos\beta\right]} \quad (15)$$

Also by substituting (12) in (6), we get:

$$T_1 = 2F_{PH} + \mu \cdot (\cos\beta) \cdot [T_1 + T_2] + F_2 \quad (16)$$

and substituting (13) in (16), yields:

$$T_1 = 2F_{PH} + \mu \cdot (\cos\beta) \cdot [T_1 + T_2] + \mu \cdot (\cos\beta) \cdot [T_2] \quad (17)$$

Now substituting (15) in (17) and solving for T_1, we get:

$$T_1 = \frac{2F_{PH}\left[1 + \frac{\mu \cdot \cos\beta}{\left(1 - \mu \cdot \cos\beta\right)}\right]}{\left[1 - \mu \cdot \cos\beta\right]} \quad (18)$$

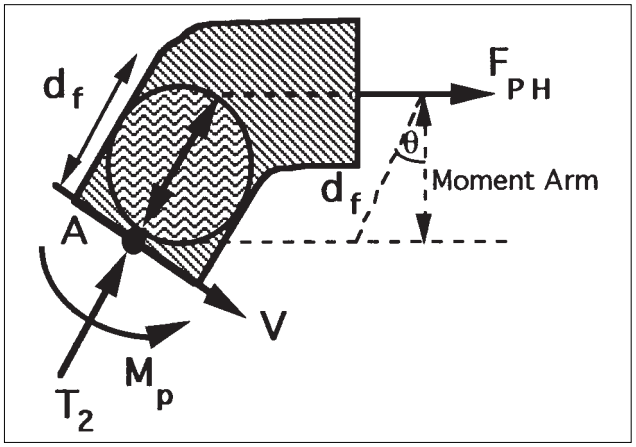

Fig. 14 - Sketch of the free body diagram of the fiber plastic hinge.

The value of F_{PH} is determined from the equilibrium of moments about point "A" in the free body diagram sketch of the fiber plastic hinge presented in Fig. 14.

$\Sigma MA = 0$ (CCW + ve)

Thus,

$$M_p = F_{PH} \cdot (\text{Moment arm} = d_f \cdot \cos\theta) \quad (19)$$

or,

$$F_{PH} = \frac{M_p}{d_f} \cdot \frac{1}{\cos\theta} \quad (20)$$

where,

M_p = Plastic moment of the steel fiber circular section, estimated as $\left(f_y \cdot \frac{\pi r_f^2}{2} \cdot \frac{d_f}{3}\right)$

d_f, r_f = the fiber diameter and radius, respectively

and

f_y = the fiber yield strength

Finally, the values of $\Delta P'$ and $\Delta P''$ can be equated to the values of T1 and T2 from equations (15) and (18), and by using equation (20) they can be expressed as:

$$\Delta P' = T_1 = \frac{\frac{2M_p}{d_f \cdot \cos\theta}\left[1 + \frac{\mu \cdot \cos\beta}{\left(1 - \mu \cdot \cos\beta\right)}\right]}{\left[1 - \mu \cdot \cos\beta\right]} \quad (21\text{-a})$$

or,

$$\Delta P' = T_1 = \frac{\frac{f_y \pi r_f^2}{3 \cdot \cos\theta}\left[1 + \frac{\mu \cdot \cos\beta}{\left(1 - \mu \cdot \cos\beta\right)}\right]}{\left[1 - \mu \cdot \cos\beta\right]} \quad (21\text{-b})$$

and,

$$\Delta P'' = T_2 = \frac{\frac{M_p}{d_f \cdot \cos\theta}}{\left[1 - \mu \cdot \cos\beta\right]} \quad (22\text{-a})$$

or,

$$\Delta P'' = T_2 = \frac{\frac{f_y \pi r_f^2}{6 \cdot \cos\theta}}{\left[1 - \mu \cdot \cos\beta\right]} \quad (22\text{-b})$$

Typical Analytical Results

For a typical Dramix steel fiber; d_f = 0.5 mm (0.0196"); $\theta = 45°$, $\beta = 67.5°$, f_y = 130 ksi (130,000 psi), and $\mu = 0.5$, we get:

$$\Delta P' = T_1 = 3.05\left(F_{PH}\right) = \frac{3.05}{\cos\theta}\cdot\left(f_y\cdot\frac{\pi r_f^2}{6}\right) \qquad (23)$$
$$= 0.0002169\cdot f_y = 28.2 \text{ lb}$$

and,

$$\Delta P'' = T_2 = 1.24\left(F_{PH}\right) = \frac{1.24}{\cos\theta}\cdot\left(f_y\cdot\frac{\pi r_f^2}{6}\right) \qquad (24)$$
$$= 0.0000818\cdot f_y = 11.5 \text{ lb}$$

Since steel applies very high local pressure on concrete at points of plastic hinges, concrete usually undergoes some extent of local crushing at these points. The local crushing will change the original value of β. Hence, it should be noted that β = 67.5° is an assumed value in the current study.

In Table 4, the mechanical contribution of the hook was derived from experimentally measured data for two different embedded fiber lengths, with the same yield strength and hook geometry (Fig. 15). In addition, the matrix strength (composition) was varied also, but this only affected the elastic bond properties and hence the pull-out load value at the onset of debonding. In all cases the value of ΔP' (hook contribution due to two plastic hinges) was reported to be about 27.5 lb. as the average of (26.7 and 28.3 lb.). The computed value of ΔP' from the analytical model is 28.2 lb., suggesting a surprisingly accurate prediction. Therefore, it can be concluded that for the same hook geometry, fiber diameter, and yield strength, the maximum pull-out load of the hooked steel fiber can be determined by adding the value of ΔP' to $\mathbf{P_1}$ (the pull-out force at onset of complete debonding). Similarly, the post peak pull-out load can be computed by adding ΔP" to the pull-out load remaining after debonding of the fiber. Here it is taken equal to $\mathbf{P_1}$. This is true if the matrix strength did not deteriorate during the straightening of the fiber hooked end.

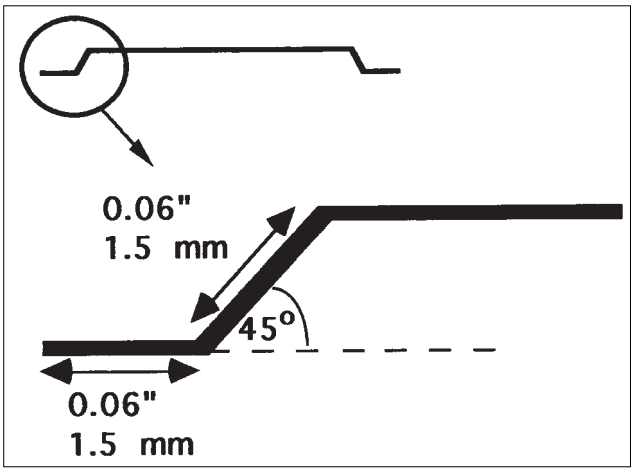

Fig. 15 - Detailing of hook geometry.

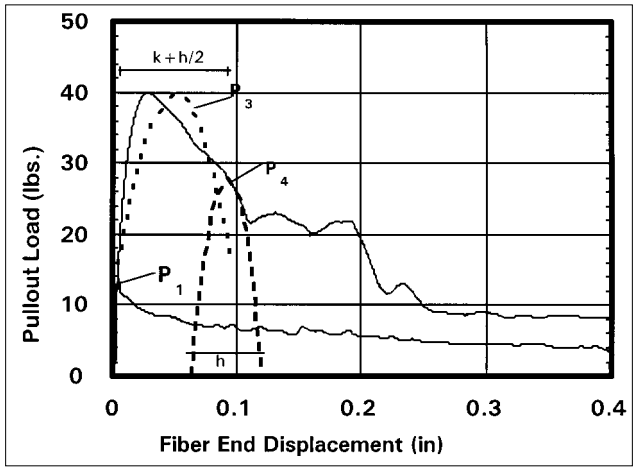

Fig. 16(a) - Two-Parabolas Smoothing Approach Plot: Comparison with Experimental Graphs for Hooked and Smooth Fibers.

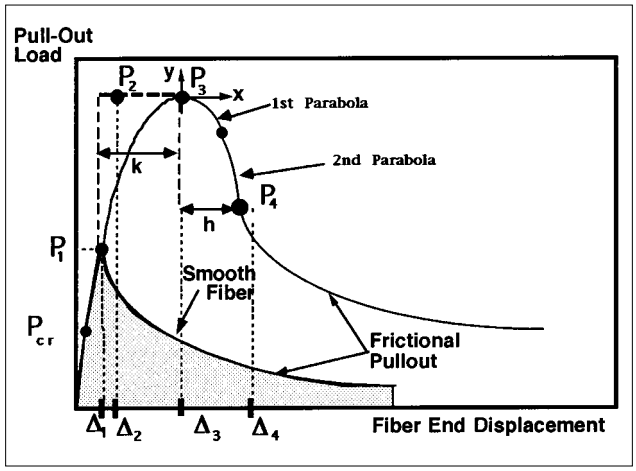

Fig. 16(b) - Schematic sketch of the assumed second degree polynomial pull-out curve of a hooked steel fiber from a cementitious matrix.

Smoothing the plastic hinge contribution

Fig. 12 illustrates a fictitious pull-out load versus slip curve assuming the contribution of the plastic moments exists and/or disappears instantaneously; it is modeled like a step function. In reality the process is transitional and continuous. To provide a more realistic transition, it is suggested that the transition between the pull-out load value P_1 to the maximum load value at P_3 and up to the post peak load value at P4 be modeled as a second degree polynomial (Parabola) with the maximum vertex at point (Δ_3,$\mathbf{P_3}$). This is an empirical smoothing approach. Several approaches were tried. One of them seemed to give reasonable results. It assumes two parabolas, the first parabola passes by P3 and spans the distance (k + h/2) symmetrically. The second parabola starts at distance (k+h/2) and spans the distance h symmetrically with vertex at P4 [see Fig. 16 (a) and (b)]. Figs. 17 - 18 show comparison plots between model

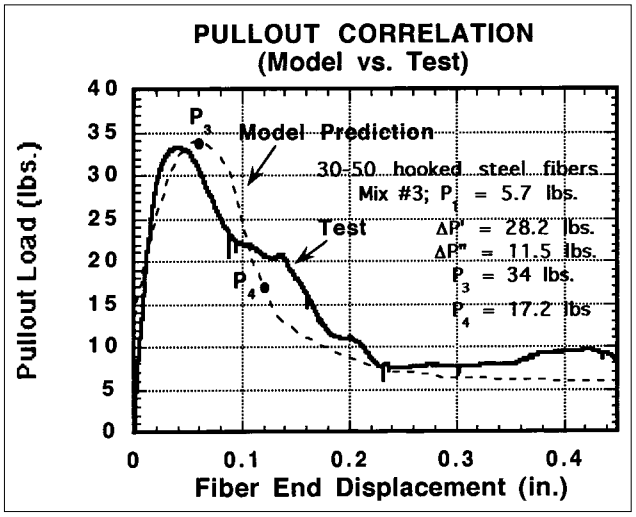

Fig. 17 - Comparison between analytically predicted and experimentally measured pull-out curves of 30 mm hooked steel fibers.

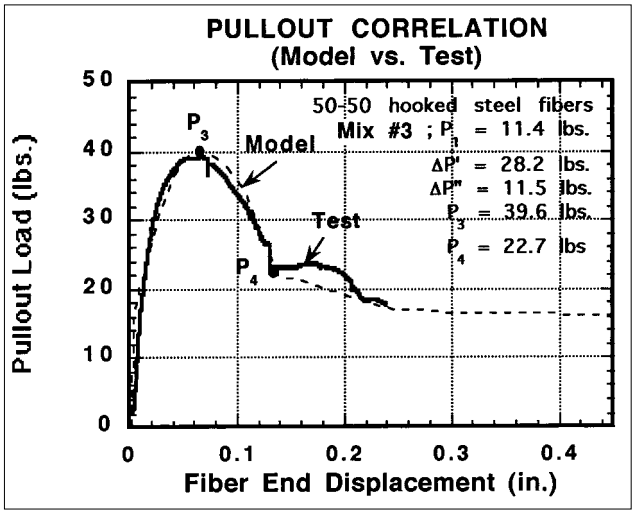

Fig. 18 - Comparison between analytically predicted and experimentally measured pull-out curves of 50 mm hooked steel fibers.

predictions and experimentally measured pull-out curves for mix#3. A good correlation can be observed in key values of pull-out loads and slips and in the general shape of the curve, providing some confidence in the model. Additional experiments may be needed to fine tune the predictions to accommodate other variables.

CONCLUDING REMARK

Prior studies have dealt with modeling the pull-out load versus slip response of a smooth fiber from a cement or ceramic based matrix, up to complete debonding [1-3, 15]. The effects of different bond parameters such as the maximum shear strength, the frictional shear stress, the bond stiffness, and bond degradation during pull-out, were considered and extensively evaluated.

In this study, a new model is developed to simulate the mechanical contribution of a fiber end "hook" to the pull-out load versus slip response of a fiber pulling out from a cement or ceramic matrix. The model is based on the concept of a frictional pulley along which the rotational resistance of up to two plastic hinges is integrated. The mechanical contribution of the hook is a function of the cold work needed to straighten the fiber as it is being pulled-out from its print. It is directly related to the hook geometry, fiber diameter, and yield strength of the fiber. The model assumes that there is no degradation in the matrix strength, or crumbling failure at the frictional contact point between the matrix and the fiber. Such an assumption holds for high strength or high performance matrices. An ongoing study is currently being carried on which addresses the shear failure of the concrete key. Analytical solutions for the maximum pull-out load value, and post-peak load values are derived. A very good agreement is observed between analytical predictions and the experimental measurements. Since the energy absorbed by composites is generally proportional to the pull-out energy of the reinforcing fibers [15-19], the model can be used as a design tool to optimize the fracture energy of fiber reinforced cement and ceramic based composites.

ACKNOWLEDGEMENT

This research was supported in part by a grant from the National Science Foundation to the NSF Center for Advanced Cement Based Materials. The center is a consortium of five institutions: Northwestern University, University of Illinois at Urbana Champaign, University of Michigan, Purdue University, and the National Institute of Standards and Technology. Any opinions, findings and conclusions expressed in this study are those of the authors and not necessarily reflect the views of NSF or the ACBM center.

REFERENCES

[1] Naaman, A. E., Namur, G., Najm, H. and Alwan, J. M., 'Bond Mechanisms in Fiber Reinforced Cement-Based Composites', Report No. UMCE 89-9, Department of Civil Engineering, University of Michigan, Ann Arbor, 233 p., 1989.

[2] Naaman, A. E., Namur, G. G., Alwan, J. M. and Najm, H., 'Fiber pull-out and bond slip, Part I: Analytical study', *ASCE Journal of Structural Engineering* **117** (9) (Sep. 1991) 2769-2790.

[3] Naaman, A. E., Namur, G. G., Alwan, J. M. and Najm, H., 'Fiber pull-out and bond slip, Part II: Experimental validation', *Ibid.* 2791-2800.

[4] Chanvillard, G., 'Analyse expérimentale et modélisation micromécanique du comportement des fibres d'acier tréfilées, ancrées dans une matrice cimentaire', Ph.D. Thesis, Department of Civil Engineering, University of Sherbrooke, Canada, 1992.

[5] Chanvillard, G. and Aitcin, P. C., 'Pull-out behavior of corrugated steel fibers', *Advanced Cement Based Materials (ACBM)* **4** (1996) 28-41.

[6] Bartos, P., 'Analysis of pull-out tests on fibers embedded in brittle matrices', *Journal of Materials Science* **15** (12) (1980) 3122-3128.

[7] Gokoz, U. N. and Naaman, A.E., 'Effect of strain rate on the pull-out behavior of fibers in mortar', *International Journal of Cement and Composites* **3** (3) (1981) 187-202.

[8] Gopalaratnam, V.S. and Abu-Makhtour, H.J., 'Investigation of the Pull-out Characteristics of Steel Fibers from Mortar Matrices', Proceeding, International Symposium on Fiber Reinforced Concrete, Madras, India, Vol. 2, pp.201-211, 1987.

[9] Banthia, N., Trottier, J. F. and Pigeon, M., 'Fiber Pull-out Mechanisms: Effects of Fiber Geometry, Loading Rate and Sub-zero Temperatures', Fibre Reinforced Cements and Concretes: Recent Developments, Elsevier Applied Science, Ed. R. N. Swamy, pp. 136-145, 1989.

[10] Bentur, A., Mindess, S. and Diamond, S., 'Pull-out processes in steel fibre reinforced cement', *Int. J. of Cement Composites and Lightweight Concrete* **7** (1) (1985) 29-37.

[11] Wang, Y., Li, V.C. and Backer, S., 'Modeling of fiber pull-out from a cement matrix', *Ibid.* **10** (3) (1988) 143-149.

[12] Li, V. C., Wang, Y. and Backer, S., 'Effect of inclining angle, bundling, and surface treatmenton synthetic fiber pull-out from a cement matrix', *J. Composites* **21** (2) (1990) 132-140.

[13] Li, V. C., Wang, Y. and Backer, S., 'A micromechanical model of tension softening and bridging toughening of short random fiber reinforced brittle matrix composites', *J. of Mechanics and Physics of Solids* **39** (5) (1991a) 607-625.

[14] Li, V. C., Wang, Y. and Backer, S., 'Fracture Energy Optimization in Synthetic Fiber Reinforced Cementitious Composites', MRS proceedings, vol. 211, Fiber Reinforced Cementitious Materials, Ed. S. Mindess and J. Skalny, 1991b, pp. 63-70.

[15] Alwan, J. M., Naaman, A. E. and Hansen, W., 'Pull-out work of steel fibers from cementitious composites: Analytical investigation', *Cement and Concrete Composites* **13** (4) (1991) 247-255.

[16] Tjibtobroto, P. and Hansen, W., 'Model for predicting the elastic strain of fiber reinforced composites containing high volume fractions of discontinuous fibers', *ACI Materials Journal* **90** (2) (March/April 1993) 134-142.

[17] Tjibtobroto, P. and Hansen, W., 'Tensile strain hardening and multiple cracking in high performance cement based composites containing discontinuous fibers', *Ibid.* (1) (January/February 1993) 16-25.

[18] Bentur, A. *et al.*, 'Chapter5: Fiber-Matrix Interfaces' in 'High Performance Fiber Reinforced Cement Composites II', RILEM Proceedings 31, E. and FN Spon, A. E. Naaman, and H.W. Reinhardt, Editors, 1996, pp. 149-191.

[19] Naaman, A.E. and Najm, H., 'Bond-slip mechanism of steel fibers in concrete', *ACI Materials Journal* **88** (2) (April 1991) 135-145.

APPENDIX I – PULL-OUT MODEL OF SMOOTH STEEL FIBERS FROM CEMENTITIOUS MATRICES

The pull-out force of smooth aligned short fibers are computed based on pull-out load versus fiber end displacement models developed by Naaman *et al.* [2-3]. The pull-out load versus fiber end displacement relationship can be summarized in the following equations. In the pre-critical and partial debonding regions, the pull-out load P is given as:

$$\mathbf{P} = \tau_f \psi u + \frac{\tau_{\max}}{\lambda} \frac{1 - e^{-2\lambda(l-u)}}{\frac{2}{Q} e^{-\lambda(l-u)} + \left(1 - \frac{1}{Q}\right)\left(1 + e^{-2\lambda(l-u)}\right)} \qquad \text{(A1)}$$

and the corresponding fiber end displacement Δ is given by:

$$\Delta = \frac{\left\{ \begin{array}{l} P(Q-1)u - \frac{\tau_f \psi u^2}{2}(Q-2) + \\ \left(P - \tau_f \psi u\right) \frac{1 - e^{-\lambda(l-u)}}{1 + e^{-\lambda(l-u)}} \frac{Q-2}{\lambda} - \tau_f \psi u l \end{array} \right\}}{A_m E_m} \qquad \text{(A2)}$$

where,

τ_{max} = maximum elastic bond strength at the fiber-matrix interface

τ_f = frictional bond stress at the fiber-matrix interface

u = debonded length of fiber

ψ = fiber perimeter

$Q = (A_m E_m + A_f E_f)/A_m E_m$

and,

$$\lambda = \sqrt{\frac{\psi \kappa}{A_m E_m}\left[1 + \frac{A_m E_m}{A_f E_f}\right]}$$

in which A_m, A_f, E_m, and E_f are the matrix and fiber cross-sectional areas and elastic moduli respectively, and k is the interfacial bond modulus.

In the pull-out region after complete debonding of the fiber-matrix interface, the pull-out load P is given by

$$\boldsymbol{P} = \psi \tau f_d(\Delta) \,.\, (l - \Delta) \qquad \text{(A3)}$$

where (l - Δ) is the length of fiber remaining embedded for any slip Δ, and $\tau_{f_d}(\Delta)$ is the frictional shear stress for a slip Δ; the subscript "d" implies damage or decay. The frictional shear stress can be assumed constant for any slip Δ. However, as in real tests, it is shown to deteriorate with increasing slip, its value as derived in Naaman *et al.* [2-3] is given by:

$$\tau_{fd}(\Delta) = \tau_{fi} \frac{e^{-(\Delta-\Delta_0)^{\eta} - \xi e^{-(l)^{\eta}}}}{1-\xi e^{-(l-\Delta+\Delta_0)^{\eta}}} * \frac{1 - Exp\left(\dfrac{-2\nu_f \mu (l-\Delta+\Delta_0)}{E_f r_f \left(\dfrac{1+\nu_m}{E_m}\right) + \dfrac{(1-\nu_f)}{E_f}}\right)}{1 - Exp\left(\dfrac{-2\nu_f \mu l}{E_f r_f \left(\dfrac{1+\nu_m}{E_m}\right) + \dfrac{(1-\nu_f)}{E_f}}\right)} \quad \text{(A4)}$$

where,

Δ = relative slip of the fiber after full debonding.

Δ_o = relative slip of the fiber at end of full debonding; as a first approximation it can be taken equal to the slip at maximum load.

ξ = damage coefficient; a dimensionless constant to give the analytical descending branch of the bond shear stress versus slip curve the same decaying trend as the experimental one.

μ = friction coefficient of the fiber-matrix interface.

ν = Poisson's ratio, with subscript f for fiber and m for matrix.

η = coefficient describing the exponential shape of the descending branch of the bond shear stress versus slip curve; for smooth steel fibers, a value of 0.2 is recommended by Naaman *et al.* [2-3].